Development and Evaluation of a UWB-Based Indoor Positioning System for Underground Mine Environments

Moritz Ziegler[1] · Amir Ehsan Kianfar[1] · Tobias Hartmann[1] · Elisabeth Clausen[1]

Abstract

Accurate positioning information is a central step in the process of increasing automation and digitalization in the mining industry. Underground mine environments are prime examples for GNSS-denied environments that pose several additional challenges for the employed indoor positioning system (IPS). This work presents an ultra-wideband (UWB)–based system specifically tailored for underground mine environments. Initially, the UWB technology is reviewed and basic concepts of IPS are explained. Both software and hardware are described in detail, including positioning algorithms, electrical circuitry, and the mining-compatible enclosure. Finally, the results from field tests in an underground mine are presented and positioning performance and the influence of dilution of precision (DOP) on positioning results are empirically evaluated. The results show that the localization errors are mostly below 1 m. Individual zones of high localization errors are suspected to be caused by noise interference. Significant DOP influence due to the mining drift geometry can be confirmed. The system shows promising localization results for different mining applications, while influences negatively impacting the accuracy are presented as items for future research.

1 Introduction: Indoor Positioning in Mining

Indoor positioning is a well-recognized challenge in GNSS-denied environments or in applications which require higher accuracy than global navigation satellite systems can provide. A leading example of environments with no satellite coverage is underground mines. With the automation and digitalization of mining processes progressing, accurate indoor positioning systems (IPS) are required, which also need to fulfil the additional constraints imposed on systems in underground applications [1]. Technical systems used in mining environments are often exposed to mechanical stress or shock, moisture, vibration, heat, and dust. In the special case of radio-based IPS, additional constraints like narrow geometries in mining drifts and signal reflection or blockage by massive rock must be considered. Spatially confined drifts only allow for sub-optimal placement of anchors,

which can lead to position inaccuracy due to dilution of precision (DOP). Signal reflection or blockage can cause noisy signals and multipath effects, which will also negatively affect positioning accuracy.

Due to its physical properties, ultra-wideband (UWB) radio seems to be a promising technology to overcome some of these challenges. UWB for positioning utilizes short pulses of high bandwidth for data transmission. This allows for accurate peak detection of the signal, thus qualifying the technology for signal propagation–based localization. In particular, the resulting resistance to multipath effects and high achievable accuracy are decisive arguments for the use of UWB.

Signal propagation positioning utilizes a signal's Time of Flight (ToF) in a medium to determine the distance between a mobile unit (tag) and a base station (anchor). In three-dimensional space, subsequent ranging with four or more anchors is required to calculate the tag's position using multilateration. While simple ToF systems require impractical time synchronization between tag and anchor, more sophisticated methods like Double-Sided Two-Way Ranging (DS-TWR) offer a way around this requirement.

✉ Moritz Ziegler
mziegler@amt.rwth-aachen.de

1 Institute for Advanced Mining Technologies (AMT), RWTH Aachen University, Wüllnerstr. 2, 52062 Aachen, Germany

This publication presents a UWB-based IPS that is specifically tailored to meet the requirements of underground mining environments. A theoretical evaluation of positioning approaches in underground mining conditions is conducted to select the applied positioning method. The development of required hardware, software and enclosure are discussed. Ultimately, tests of the implemented system in an underground mine are presented and the positioning error as well as the influence of the DOP effect are quantitatively analyzed. In Section. 2, the applications for localization technology in mining and for the specific case of underground mining are described, from which the technical requirements are then derived. The UWB technology with its physical properties, as well as possible techniques for IPS, are presented in detail in Section. 3. Section 4 then presents the system design concerning algorithms and developed hardware. The system's application in an old silver mine, Reiche Zeche, Germany, and the measurement results are described in Sections. 5 and 6, respectively. The paper concludes with a summary and outlook on future research areas in Section. 7.

2 Localization in Underground Mining

With increasing automation and digitalization in the mining industry, reliable location tracking in underground environments is a key challenge [2]. Different applications call for varying requirements. The following section covers requirements from most valuable applications and aligns general technical challenges and the state of the art of positioning in underground mining.

2.1 Application-Driven Technical Requirements

According to Clausen et al., industry experts have identified safety concerns and collision avoidance as well as process analysis and optimization as major drivers for the interest in positioning [1]. Furthermore, positioning is one of the key requirements to be fulfilled as the industry is heading towards autonomous navigation of mining equipment in complex underground environments.

Collision avoidance and safety applications aim to prevent collisions between mobile equipment, but even more importantly, between mobile equipment and people. For collision avoidance, a relative tracking or even ranging between two objects in the direct vicinity is mostly sufficient, if reliably done at a high frequency with an accuracy of decimetres. [3]

Process analysis and optimization are focused on tracking equipment over large parts of the mine. For process analysis, the exact position of the vehicle is not of primary interest, but rather the operating point, stope, or mine drift at which the equipment currently operates. Positioning errors of several metres are in this case acceptable and low update rate would be sufficient to provide information for process optimization.

While process analysis in large mining operations may allow for a higher tolerance in positioning error, process automation applications require a higher degree of confidence in positioning. Positioning in a global frame is one key requirement for autonomous mining equipment to navigate flexibly in an underground environment. Optimal and reliable performance of automated equipment requires a high degree of confidence in localization. The acceptable error in this case may be more in the dimension of few decimetres or even centimetres, depending on the concrete application.

2.2 General Technical Requirements

To fulfil these requirements from the applications, a potential technology must overcome different challenges from the geometric, mechanical, and operational properties of the operations. These challenges define further requirements for automation systems that are often considered harsh conditions.

It must be suitable to overcome the special challenges of the mining industry. Underground environments typically are spatially confined. Mining drifts usually are narrow tunnels, which only allow for sub-optimal placement of anchors and thus negatively affect positioning performance. Additionally, massive rock formations can cause significant multipath effects due to signal reflection. None-line-of-sight (NLOS) situations between tag and anchor might heavily impact positioning performance or lead to loss of signal.

The developed hardware also needs to be adjusted to the mining environments. Hardware in underground mining is often exposed to dust, heat, and moisture, especially if used in the production zones of the mine. Material handling processes or rockfall causes mechanical shock or vibration, all of which needs to be considered during development of hardware and casings.

Another property taken into consideration is scalability. Firstly, the scalability of a system can be evaluated in terms of spatial coverage. For many applications, large parts of the mine must be covered by the positioning system. This can place constraints on the selected positioning technique. Secondly, scalability in terms of number of tags can be important. Tracking a high number of mobile units can be difficult with certain positioning techniques. In the mining context, however, most applications require the tracking of only a limited number of mobile units.

Finally, a system that is employed in a commercial operation always needs to be cost efficient. Equipping large parts of an underground mine with a positioning system may soon become costly and require high capital expenditure. The mining industry in general, however, is a very capital-intensive industry. Technologies, that are economically unfeasible

in the consumer sector, may be feasible in the mining industry if it leads to improved productivity and increased safety.

The resulting requirements for the positioning system can be summarized as follows:

- Accurate positioning performance
- Robustness against multipath
- Robustness against noisy signal
- Mechanical and chemical durability
- Spatial scalability

2.3 State-of-Art of Commercial Localization Technology

There are different technologies employed in indoor positioning systems using Wi-Fi, Zigbee, Bluetooth, and UWB. Compared to other technologies, UWB shows low complexity and higher accuracy. In applications like manufacturing and warehouse asset tracking, several commercial UWB-based positioning and localization systems are already available. These systems apply various localization methods, e.g. UbiSense and pozyx, which are based on Time Difference of Arrival and Time of Flight of the UWB signals, RealTrack using triangulation principle, and BeSpoon using Two-Way Ranging and Angle of Arrival. [4] [5] [6]

For underground mines however, UWB is seldom applied on a commercial scale. Zare et al. focus their review on IPS mainly on Wi-Fi-based systems, while UWB is only very briefly covered. Among a list of 20 commercially available localization solutions for the mining industry, only two are based on UWB, one of which is a hybrid solution. This is even though UWB provides the best localization results among the works reviewed. [7]

2.4 Literature Review

In recent publications that reviewed localization technology in underground mining, UWB systems often are hardly considered. Zare et al. find that UWB plays a minor role among commercial IPS in the mining industry and thus, UWB is hardly covered in their work (Section. 2.3) [7].

Seguel et al. perform a review of scientific works on underground mine positioning. Among almost 50 publications that are reviewed, only three publications deal explicitly with UWB positioning, while two more deal with hybrid solutions involving UWB. Remarkably, the five publications involving UWB which are considered in their review are among the most accurate. The authors' requirements however are based on the MINERS-Act of 2006, which requires 60.96 m of error or less as minimum accuracy for underground positioning systems. Good results in accuracy are therefore not the focus of that research effort. [8]

Nonetheless, UWB positioning in underground scenarios has been examined in several scientific publications. Some of these publications briefly described in the following explicitly consider difficult conditions like NLOS. However, the experiments presented are either conducted only in laboratory environment or they do not demonstrate a full positioning solution. Moreover, another focus of this article is to present the development of a complete UWB positioning system. Several publications on the development of UWB systems are therefore referenced in the following.

Barua et al. conduct a performance study on UWB ranging in underground scenario. The experimental setup is an underground mine in which Two-Way Ranging operations are performed. LOS and NLOS situations are both explicitly compared, showing ranging error below 0.3 m under LOS conditions and below 2 m under NLOS conditions. [9]

Cao et al. published two papers on the localization of a shearer in a longwall. Both publications explicitly deal with the frequent NLOS situations in longwall mining and they both present advanced algorithmic approaches to mitigate NLOS error. Experiments are conducted in a laboratory setting resembling the geometric conditions in a longwall mining operation. [10] [11]

Molnár et al. present the development of a UWB IPS based on Double-Sided Two-Way Ranging. The authors use commercially available development boards as UWB modules. Position estimation is done using Kalman filtered range measurements and a simple numerical optimization method to minimize the residual error. The system is tested in a small-scale laboratory setup. [12]

Ding et al. present the development of a localization system which is employed on a warehouse robot using a UWB and computer vision approach. Double-Sided Two-Way Ranging is used to navigate the robot to an area while precise positioning is then done via a computationally intensive computer vision approach. [13]

Li et al. present a system for six degree of freedom localization of a mobile platform in underground coal mines, which fuses UWB and inertial measurements (IMU). The authors give a detailed description of their algorithmic approach and the systems architecture. The system is simulated and validated extensively in real world testing in an underground mine environment. Furthermore, a relationship between geometrical anchor setup and localization performance is formulated. According to this, rectangular anchor setups with a side ratio of 2:1 or less are optimal. [14]

The development of the current research in comparison to the existing publication on UWB system development and positioning in mine environments is described as follows:

- The research presented gives a comprehensive and detailed description of all the system components, especially UWB hardware. The novel PCB is an improved

version of the one presented in [3] and electronic parts and circuitry are described in detail. Previous research often use commercial UWB development kits [12] or modules [13] [14] and do not develop custom UWB PCBs.

- Testing is conducted in very difficult environment in terms of anchor geometry, signal reflection, and bad signals from distant and/or NLOS anchors. The systems presented in [12] and [13] are tested in small scale under controlled laboratory conditions. In [14], extensive tests are conducted in a real-world underground scenario, yet the experimental setup still creates favourable conditions for IPS in terms of LOS and anchor geometry. Almost all mentioned research use rectangular setups of the minimum required number of anchors (four) with the tag more or less in the centre. Of the presented publications, only [9] explicitly considers NLOS situations in a real underground scenario and only for simple range measurements. The publications [10] and [11] consider mixed LOS and NLOS scenarios, but only in lab scale and not in challenging underground environment. In the current research, however, tests were conducted in a highly suboptimal setup in an uncontrolled environment to test the system and technology capabilities under extreme conditions.

- The influence of the sub-optimal anchor configuration, as it is dictated by the test environment, is investigated. In [14], the influence of anchor positions is briefly discussed and conditions for an optimal setup are formulated. Similar optimum criteria are formulated in [15]. In the current research, the test setup clearly violates the optimum criteria. The resulting influence on the test results are therefore quantified in form of Dilution of Precision (DOP) values over the course of the measurement. Additionally, the behaviour of DOP value and measurement error in general and along different directions is investigated.

The feasibility and basic ranging functionality of the systems predecessor has already been demonstrated in [3] with respect to collision avoidance. The system has since been improved in software and hardware and is now presented as a solution for underground positioning.

3 Ultra-Wideband

Over the last decades, the ultra-wideband (UWB) technology, with its defined characteristics, has shown some notable advantages over other radio technologies in the field of indoor positioning. In the following sub-sections, the frequency band of UWB is described, and its advantages and disadvantages are discussed.

3.1 Regulations and Standardization

Ultra-wideband (UWB) signals characteristically make use of a large frequency band within the electromagnetic spectrum. In 2002, the U.S. Federal Communications Commission committed regulations to license-free use of UWB. This made the frequency band from 3.1 to 10.6 GHz available for unlicensed operations in UWB technology. Until today, many other countries as well as the European Union have approved the rules defining UWB as a license-free frequency band. [16] [17] The UWB frequency band is defined by the European Union to range from 3.8 to 4.2 GHz as well as from 6 to 8.5 GHz. [18]

The physical layer (PHY) and medium access control layer (MAC) of UWB communication are standardized according to IEEE 802.15.4 and can be found in [19]. Both PHY and MAC standardization offer support for accurate ranging. IEEE 802.15.4 defines Impulse Radio UWB as PHY for UWB with in total 16 different channels, twelve of which possess bandwidth of 499.2 MHz and four of which possess higher bandwidth of 1000 MHz. The higher bandwidth channels are especially suitable for ranging as they offer longer communication range, enhanced multipath resistance, and more accurate ranging results. The PHY's mandatory ranging capabilities according to IEEE are the ranging counter and the figure of merit. The IEEE defined MAC offers timestamp report to enable accurate ranging. [19]

According to the part 15 of the FCC regulations, the Effective Isotropically Radiated Power of -41.3 dBm per MHz and the -10 dB level of emissions in the license-free band may be used in the USA and EU countries [20]. For more information on the technical requirements for indoor and handheld UWB systems, see Sects. 15.517 and 15.519 of the Code of Federal Regulations 47 (CFR47), and Sect. 15.521 on the applicable technical requirements for all UWB equipment or the regulations of the European Telecommunications Standards Institute (ETSI) [21] [18].

3.2 Properties of UWB Radio Signals

Not every signal in the above-mentioned frequency band belongs to UWB, as UWB signals must span a bandwidth of at least 500 MHz and have a central frequency (f_c) of above 2.5 GHz. Equation 1 and Fig. 1 depict the calculation of the central frequency,

$$f_c = \frac{f_L + f_H}{2} \tag{1}$$

Fig. 1 The central frequency of UWB spectrum according to its high and low frequencies (modified from [22])
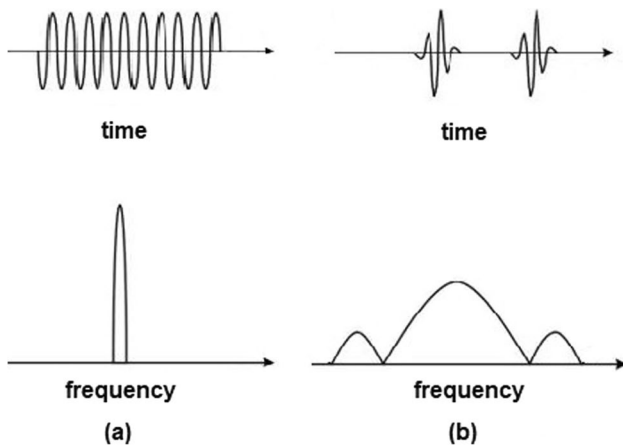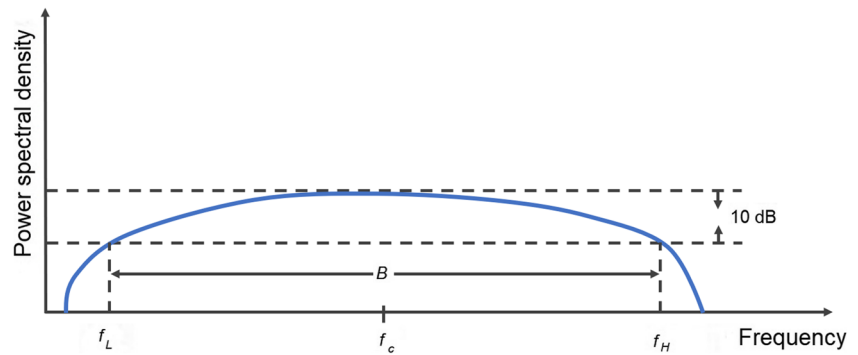

Fig. 2 **a** Continuous wave signal and **b** UWB signal in time and frequency domains (modified from [6])

where f_L and f_H are the low and high frequencies. [22] UWB signals have some physical and inherent properties that make them suitable for some special applications such as indoor positioning. Compared to continuous wave signals, UWB signals are large in the frequency domain but short in the time domain, as shown in Fig. 2.

The short length of the UWB signal in time domain protects it against interferences with noise and, in the event of signal attenuating multipath effects, the reflected signals will not interfere the original signal. The immunity to noise and multi-pathing causes UWB to be the focus of research in a wide range of applications. High speed communication, low power consumption, and scalability are its other inherent properties [23]. The accuracy of the positioning methods using UWB is higher compared to the other technologies such as Wi-Fi and Bluetooth, which has made it the focus of recent research in the field of indoor positioning [24]. Its short signal duration in time domain provides higher accuracy in positioning, as it provides a higher time resolution that helps the signal detector detect the signal in one point at its peak.

3.3 UWB Technology in Indoor Areas

Due to the above-mentioned characteristics of UWB such as its resistance to multipath and noise, and its low power consumption and high accuracy, it is a suitable technology for applications such as indoor positioning. The main barriers to indoor communications, especially in underground mines, are the narrow passageways that cause multipath propagation of signals. Also, the electromagnetic noise emanating from the machines and other communication systems in the mine can be a problem for an IPS. As mentioned earlier, UWB is resistant to multipath and largely immune to noise, so it can be used as a suitable technology for indoor positioning. Since the galleries in an underground mine are narrow in width and there are many barriers to the signals, such as the mining machines and personnel, a highly accurate positioning technology like UWB is required.

3.4 Positioning Methods Using UWB

Radio-based IPS makes use of different physical properties of the signal propagation to determine a position from a measured signal. There are various positioning methods used by UWB for localization, which can be categorized into the following techniques: Received Signal Strength (RSS), Time of Flight (ToF), Time Difference of Arrival (TDoA), and Angle of Arrival (AoA). Brief reviews of the mentioned methods are given in the following sub-sections.

3.4.1 Received Signal Strength

Received Signal Strength (RSS) is a localization technique that utilizes the measured signal strength at the receiving radio set to infer the distance between the transmitter and receiver.

Since the signal strength parameter is available with a lot of radio technology systems, the RSS method is easily implemented and has become a popular choice among low-cost positioning systems [25]. However, one major drawback of this technique is that signal strength behaviour is often

not deterministic [2]. Fingerprinting algorithms are a way to overcome this problem, but the technique remains sensitive to multipath effects and changes in the environment. With this method of positioning, barriers to the signals such as the mining machinery, mine profiles, and rocks can completely block or severely attenuate the signals, which can lead to errors in position determination, since the available power at the receiving antenna is proportional to the square of the distance over a range in a time-harmonic free-radio system. [25]

3.4.2 Angle of Arrival

Angle of Arrival (AoA) techniques measure the angle of the incoming signal relative to the measuring station. This requires an array of antennas on the receiving radio set that records the time difference of the incoming signal between the individual antennas, so an angle can be determined. In three-dimensional space, the angle measurement with three anchors is sufficient to obtain a single position using triangulation. This technique however is not very suitable for long distances, since a small error in the measured angle will cause a large error in distance estimation. [25]

3.4.3 Time Difference of Arrival

Time Difference of Arrival (TDoA) methods are used to calculate the position of the tag based on the difference of arrival times at the anchors. The underlying physical property of the signal is the known propagation speed.

In multilateral TDoA, the tag sends out a short signal referred to as a blink, which is received at the anchors. The difference in arrival time between the anchors results in range differences, representing the difference of the distances between the tag and two anchors. In a geometric sense, the TDoA measurements result in hyperbolas that describe the possible locations of the tag based on the measurement of two anchors.

Figure 3 shows the TDoA localization of a tag in two-dimensional space. With three anchors, two independent range differences can be determined which is sufficient for unambiguous localization. The position of the tag lies in the intersection point of the hyperbolas. For localization in three-dimensional space, a fourth anchor is required.

While the TDoA approach does not require clock synchronization between anchors and tag, it does however require the clocks of the anchors to be synchronized. This aspect poses the main drawback of TDoA systems since cable-bound clock synchronization between the anchors reduces flexibility and increases the costs of the system. Wireless synchronization as described in [26] on the other hand significantly increases the complexity of the required algorithms.
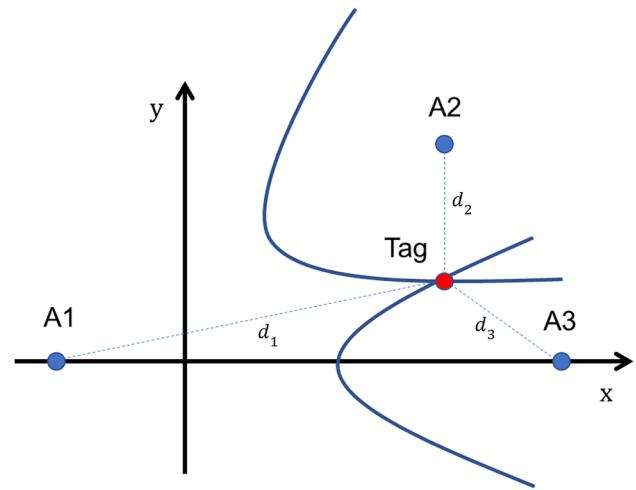

Fig. 3 Graphical representation of TDoA measurements based on three anchors (A1–A3)
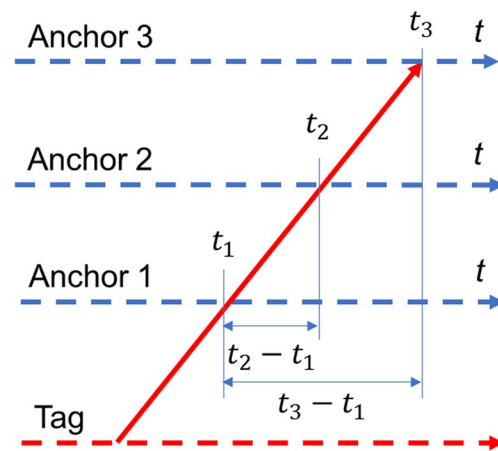

Fig. 4 Message scheme of TDoA approaches. A single blink is sufficient for localization

Figure 4 shows the messaging scheme in a TDoA approach. It is evident that only a single blink is required to estimate the tag's position, which results in low energy consumption. Furthermore, no inherent processing times at the anchors are required, so anchor blockage is minimal. One of the main advantages of TDoA technique is thus increased scalability compared to TWR techniques. [25]

3.4.4 Time of Arrival and Two-Way Ranging

Time of Arrival (ToA) approaches exploit the known propagation time of a signal in the medium to calculate the distance between transmitter and receiver. This process is called ranging. After ranging with a sufficient number of anchors, the position of the tag can be determined by multilateration.

The straightforward ToA approach is to subtract the timestamp of the emitted signal t_0 from the timestamp of signal reception t_i and multiply it by the propagation speed c to obtain the distance d_i between transmitter and receiver:

$$d_i = c \cdot (t_i - t_0) \tag{2}$$

Based on one measurement, all possible positions of the tag are located on an orb with radius d_i and the centre coordinates (x_i, y_i, z_i). This holds for three-dimensional space. For the sake of readability, the following equations are reduced to the two-dimensional case, in which the spheres of possible positions are reduced to circles. The extension of the equations into three dimensions is straightforward. The Euclidean distance d_i between tag (x_0, y_0) and anchor (x_i, y_i) is expressed by the following equation:

$$(x_0 - x_i)^2 + (y_0 - y_i)^2 = d_i^2 \tag{3}$$

As there are two unknowns (x_0, y_0) in Eq. 3, ranging with two anchors could lead to a unique solution in the optimal case. This is, if the tag was located on the direct line between
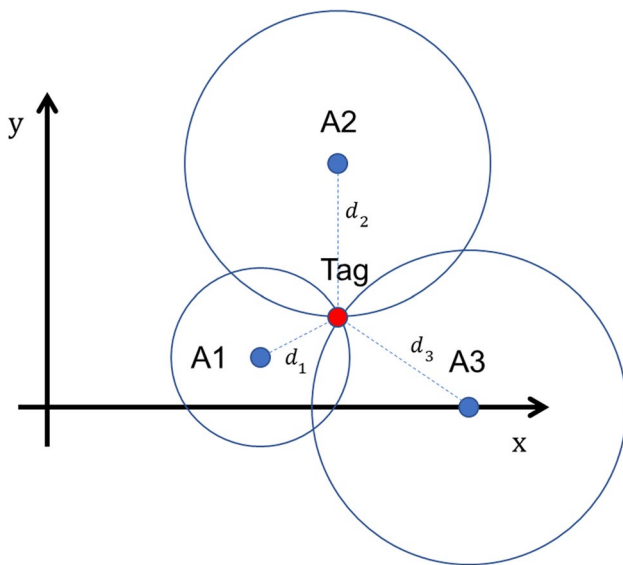
the two anchors. Since this is usually not the case, ranging with two anchors will generally produce two possible locations at the intersection point of the two ranging circles. Thus, in two-dimensional space at least three anchors are required to obtain a single, unambiguous position of the tag, while four anchors are required in three-dimensional scenarios. Figure 5 depicts the position of the tag at the intersection point of the three range circles.

$$
\begin{aligned}
(x_0 - x_1)^2 + (y_0 - y_1)^2 &= d_1^2 \\
(x_0 - x_2)^2 + (y_0 - y_2)^2 &= d_2^2 \\
&\vdots \\
(x_0 - x_i)^2 + (y_0 - y_i)^2 &= d_i^2
\end{aligned}
\tag{4}
$$

The above approach however requires accurate time synchronization between anchors and the tag which proves difficult in practice. One approach to avoid the requirement of time synchronization is Two-Way Ranging (TWR). The most straightforward variant of TWR techniques is Single-Sided Two-Way Ranging (SS-TWR). In this approach, the tag sends out a ranging signal and waits for the respective anchor to answer. Sequential SS-TWR with multiple anchors (Fig. 6) yields the required ranges for positioning.

A more sophisticated approach than SS-TWR is Double-Sided Two-Way Ranging (DS-TWR). After the initial ranging process, another signal exchange is added, resulting in two range measurements of which the mean is used to perform the multilateration process. Errors in the range measurements (i.e. due to clock drift) are thus smoothed out. This is explained in detail by Zandian [25]:

Figure 7 shows the sequential ranging process in the DS-TWR approach. In the shown scenario, the calculated propagation time is passed back to the tag in a feedback message. The individual travel times T_1 and T_2 for both roundtrips can be calculated according to Eq. (5).

$$T_i = \left(\frac{t_i - t_{ti}}{2} \right) \tag{5}$$

With the elapsed times t_1 and t_2, the known turnaround times t_{ti}, and the propagation speed c of the signal in the medium, the distance between anchor and tag can be calculated according to Eq. (6).

Fig. 5 Graphical determination of position by (tri-)lateration between tag and anchors A1–A3. The solution to the set of Eq. (4) shown below yields the position of the tag

Fig. 6 SS-TWR schematic. During the turnaround time, the anchor is blocked from communication with other tags, so scalability of the method is limited
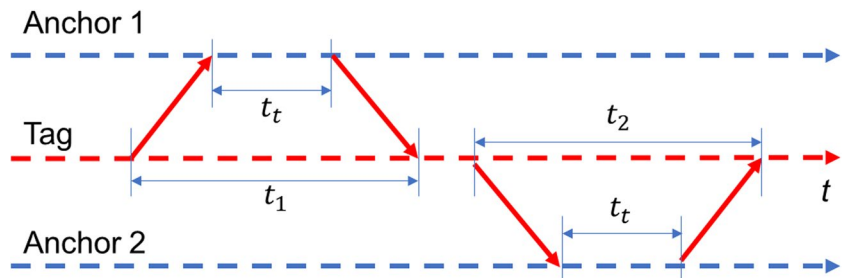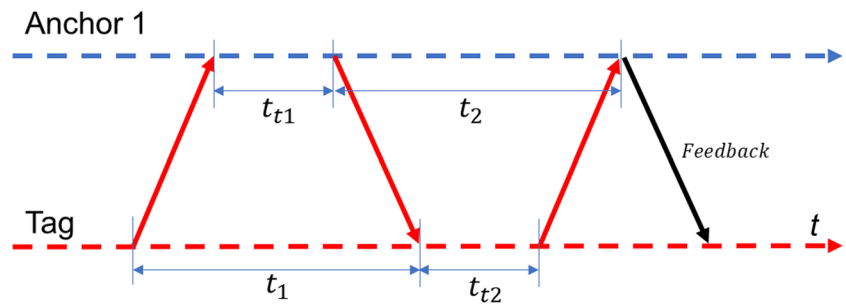
Fig. 7 Messaging scheme of DS-TWR. Errors in ranging are smoothed out by multiple message exchanges

$$d_1 = \frac{(T_1 + T_2)}{2} \cdot c = \left(\frac{(t_1 - t_{t1}) + (t_2 - t_{t2})}{4} \right) \cdot c \qquad (6)$$

While TWR techniques are generally more robust to range measurement errors, one of the major drawbacks is the scalability of the system. For unambiguous position estimation, ranging with at least four different anchors is required. Figure 7 shows how at least three, four including feedback, messages must be exchanged per anchor, resulting in at least twelve (sixteen including feedback) messages exchanged for a fully determined position update. This imposes limits on the number of possible tags due to increased air traffic and anchor blockage during turnaround times. Additionally, since more messages need to be exchanged per ranging, the energy consumption of TWR is higher than for TDoA. [25]

3.4.5 Evaluation of Positioning Methods for Underground Applications

The described methods require careful evaluation regarding their suitability for underground application. From the prior determined requirements localization accuracy, multipath (and noise) resistance and cost can be considered relevant. Furthermore, the number of needed tags for localization, special scalability, and needed algorithmic complexity must be considered when designing and implementing a UWB IPS.

Table 1 assesses the positioning methods based on the requirements formulated in Section. 2.2. The different localization techniques are evaluated as + (favourable) and − (unfavourable) with regard to defined criteria. The selected categories are furthermore weighted according to their relevance based on practical experience and in line with [27].

The most prominent property of a localization system is almost always the localization accuracy. Beyond that, multipath effects are expected to be the most challenging aspect of spatially confined mining environments. Both of these aspects speak in favour of signal propagation–based methods (TWR, TDoA), as AoA and Received Signal Strength Indication (RSSI) are very susceptible to multipath effects. TDoA and TWR additionally benefit from accurate peak detection, which is an inherent advantage of the UWB radio technique. TDoA systems are subject to a trade-off between hardware complexity and cost versus algorithmic complexity. Cable-bound synchronization on the one hand increases hardware complexity and cost, while also impairing the spatial scalability of the setup. Wireless synchronization on the other hand requires an additional complex algorithmic component for clock management like the ones proposed by McElroy et al. in [26]. Lastly, energy consumption is higher for TWR systems compared to TDoA. With the application in mind, the energy consumption of the tag is not critical since it will be mounted on a vehicle with available power supply. For the stationary anchors, most applications (in which anchors are deployed more than a few days) require an external power supply anyways.

Consequently, TDoA systems are particularly suited to situations where many nodes need to be monitored on

Table 1 Comparison of localization techniques regarding pre-defined evaluation criteria (in line with [27]). The criteria are evaluated as favourable (+) and unfavourable (−) with respect to the given application

Criteria	TWR	TDoA	RSSI	AoA	*Relevance*
Localization accuracy	+	+	−	+ (Short distance)	High
Multipath resistance	+	+	−	−	High
Number of tags	−	+	+	+	Low
Cost	+	−	+	−	Medium
Spatial scalability	+	Trade − off	+	+	Medium
Algorithmic complexity	+	Trade − off	−	+	Medium
Energy consumption	−	+	+	+	Medium

limited space, and where low energy consumption (e.g. for person detection with battery-powered tags) is critical. In the mining context, this could potentially apply to highly frequented areas like crushers or the shaft, rather than covering extensive parts of the mine drifts. For these reasons, the DS-TWR method has ultimately been chosen for the system presented in this publication.

3.5 DOP Influence in Underground Environment

The Dilution of Precision (DOP) effect describes the influence of ranging measurement error on the error in localization based on the geometrical anchor distribution. It is quantified using the DOP value. Derivation and detailed explanation of the DOP value can be found in [2, 15]. DOP values can be calculated in different directions (XDOP and YDOP in X and Y direction, respectively) and are derived from the matrix Q:

$$Q = \left(H^t H\right)^{-1} \tag{7}$$

Each row of the Jacobian H is derived analogous to (17) and (18) in Section. 4.1.2 for each of the recently contacted anchors. However, for this purpose, the columns of H are reduced to X, Y, and Z direction, and the velocity entries are ignored.

XDOP and YDOP values can now be directly taken from the diagonal entries in Q:

$$\begin{aligned} XDOP &= Q_{11} \\ YDOP &= Q_{22} \end{aligned} \tag{8}$$

From Eqs. (7) and (8), it becomes clear that DOP values are only dependent on the geometrical constellation of the anchors and the tag.

Figure 8 clearly shows how certain anchor distributions amplify the influence of noise in the range measurement on the positioning process for a given position.

For very narrow geometrical constellation of the anchors along one axis, the overlap of the measured pseudo-ranges is larger in the orthogonal direction, leading to a larger possible area of tag locations. Therefore, if anchors are deployed along a very narrow tunnel as it is often the case in underground mines, localization performance in perpendicular direction to the tunnel is expected to suffer. Figure 9 clarifies this behaviour.

In previous research, it is generally accepted that lowest DOP and thus optimal localization performance can be achieved, if the mobile node is located in the centre of a rectangle of anchors with a side ratio of 2:1 or less [14] or, more generally, a regular polygon [15].

For the considered application, these criteria are almost never met, and the DOP effect is thus expected to negatively impact the positioning accuracy in orthogonal direction to tunnel orientation.

4 System Design

The method of positioning determines the software and hardware structure of the modules and the whole positioning system. As mentioned before, the positioning method based on estimation of the distances between the anchors and the tag using DS-TWR is employed. According to this method, the software and hardware has been designed and developed as described in the following sub-sections.
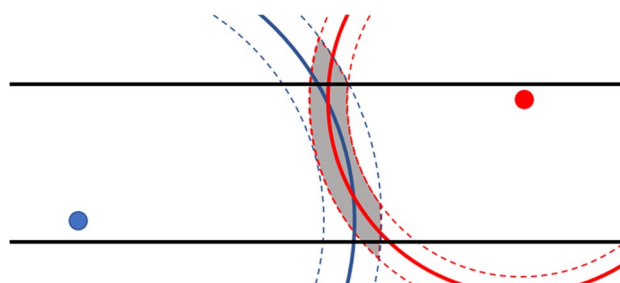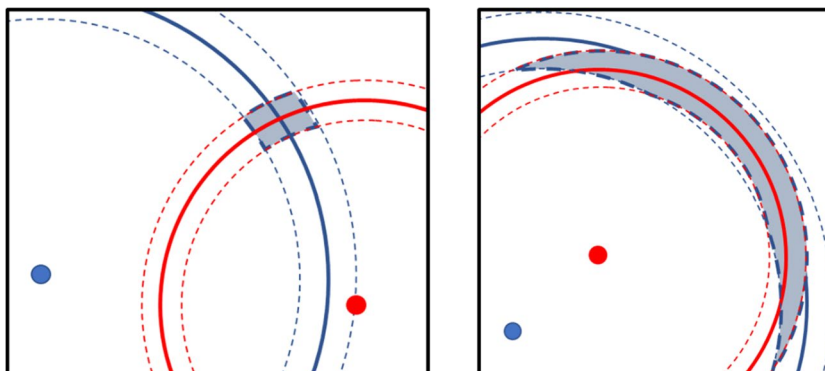

Fig. 9 DOP effect in narrow tunnels. Localization accuracy perpendicular to the tunnels main direction is decreased

Fig. 8 Schematic representation of the DOP effect. On the right, the overlap of the noisy pseudo-ranges is significantly larger, leading to a higher area of possible tag locations

4.1 Software and Algorithms

In the following sub-section, the developed software is presented in two steps. Section 4.1.1 presents the overall structure of the software and describes the different components. Section 4.1.2 gives a detailed description of the implemented multilateration algorithm and its characteristics.

4.1.1 Software Structure

The presented system consists mainly of two components: the UWB tag carrying out the DS-TWR on embedded hardware and a connected computer running the Robot Operating System (ROS) on Ubuntu 20.04. Figure 10 displays the software components in a block diagram. The DS-TWR algorithm periodically polls all anchors in the vicinity of the tag. DS-TWR ranging is performed afterwards sequentially with all contacted anchors. The raw ranging data, consisting of the calculated range and the identification of the respective anchor, is then transferred from the tag to the computer, where it is recorded and the multilateration process is carried out within the ROS framework. ROS was chosen as a development tool because it offers several convenient features such as data logging and a pub-sub-based messaging system. These features are particularly interesting during development phases since they allow for easy debugging and post-processing of recorded data. The developed system will prospectively be ported to the embedded hardware on the tag itself, which is symbolized by the blank box in Fig. 10. Computational aspects thus must be considered in the choice of the underlying algorithm. The multilateration process is therefore performed by an Extended Kalman Filter (EKF), which is implemented in ROS.

4.1.2 *DS-TWR Positioning* via *Extended Kalman Filtering*

In a mathematical sense, the process of multilateration means to solve the nonlinear equation system presented in Eq. 5. In theory, the solution can be obtained by closed analytical approaches. In practice, it is often not possible to reach a clear solution through closed-form algorithms, as measurement error and noise result in a solution space rather than a single value. It is therefore the goal of the positioning algorithm to minimize the residual error and to find the optimal solution within the solution space. [25]

As a central component of the positioning algorithm, the Extended Kalman Filter (EKF) is chosen. The EKF is a nonlinear extension of the generic Kalman Filter and is well known for positioning applications. It is known to be an effective estimator in noisy environments while at the same time possessing low computational complexity [25] [28]. The latter point is of particular interest in this case since the positioning system will potentially be deployed on embedded hardware with low computational power. The following sections provide a detailed overview of the EKF algorithm and describe the applied configurations for the given application.

The Extended Kalman Filter mainly uses two steps, the prediction step and the correction step. During the prediction step, the state of the system is anticipated based on its estimated behaviour. In the correction step, the incoming measurement is weighted according to the measurement uncertainty and applied to the predicted state. Thus, measurement uncertainty and expected system behaviour are both considered and weighed against each other in the state estimation.

In this case, the system state x_k is represented by a position-velocity model (PV model) in three-dimensional state. The velocities along the axis are denoted as $\dot{x}, \dot{y}, \dot{z}$.

$$x_k = (x, y, z, \dot{x}, \dot{y}, \dot{z}) \tag{9}$$

The state vector will be reduced to a two-dimensional state $x_k = (x, y, \dot{x}, \dot{y})$ for easier notation. Extension to three dimensions is straightforward.
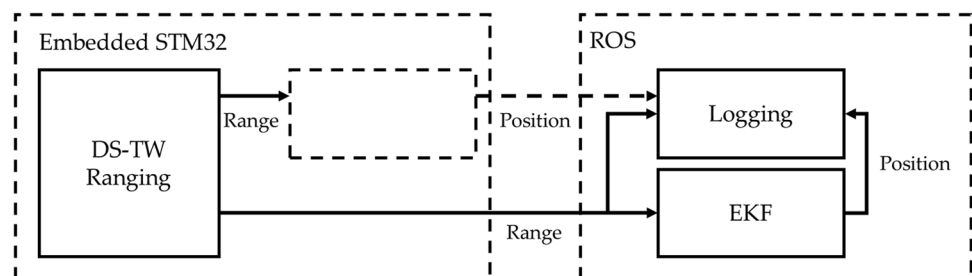
In the case of position determination using TWR, the prediction step propagates the previous position x_{k-1} to the current time step k. The result is the a priori state vector $\hat{x}_k$:

$$\hat{x}_{k|k-1} = F \cdot x_{k-1} \tag{10}$$

The transition matrix F according to the PV model is:

$$F = \begin{pmatrix} 1 & 0 & \Delta t & 0 \\ 0 & 1 & 0 & \Delta t \\ 0 & 0 & 1 & 0 \\ 0 & 0 & 0 & 1 \end{pmatrix} \tag{11}$$

Fig. 10 Block diagram of the used software components

The a priori covariance matrix $\widehat{P}_{k|k-1}$ belonging to the predicted state $\widehat{x}_k$ is determined from the previous a posteriori covariance matrix $\widehat{P}_{k-1|k-1}$ as follows:

$$\widehat{P}_{k|k-1} = F_k \cdot \widehat{P}_{k-1|k-1} \cdot F_k^T + Q \tag{12}$$

The matrix Q is the covariance matrix of the process noise. In the correction step, the a priori state vector is corrected based on the measurement z. The vector y describes the difference between the measurement z and the measurement model $h(x)$, applied to the predicted state $\widehat{x}_{k|k-1}$:

$$y = z - h\left(\widehat{x}_{k|k-1}\right) \tag{13}$$

Some EKF implementations utilize the distance measurements of four anchors simultaneously as their measurement model [28]. In this case however, the measurement model is a single Euclidean distance between the tag and an anchor i (14). The EKF step is thus performed every time a new ranging is carried out. The advantage is that no loss of information occurs if ranging with one of the four anchors fails, which would normally lead to the three obtained ranges being discarded.

$$h\left(\widehat{x}_k\right) = d_i = \sqrt{\left(x_0 - x_i\right)^2 + \left(y_0 - y_i\right)^2} \tag{14}$$

The vector y is applied to the a priori vector as described in Eq. 16:

$$\widehat{x}_{k|k} = \widehat{x}_{k|k-1} + K \cdot y \tag{15}$$

The Kalman Gain K quantifies the confidence in the measurement compared to the prediction. It is calculated as follows, where R denotes the measurement noise variance.

$$K_k = \widehat{P}_{k|k-1} \cdot H_k^T \cdot \left(H_k \cdot \widehat{P}_{k|k-1} \cdot H_k^T + R\right)^{-1} \tag{16}$$

The Jacobian H linearises the measurement function around the a priori state vector $\widehat{x}_{k|k-1}$. It results from the partial derivatives of the measurement function $h\left(\widehat{x}_k\right)$ with respect to the unknowns. It is of the dimension $n \times m$, with

m being the number of elements in the state vector. The number of rows n is equal to the number of values in the measurement. Hence, in this case the Jacobian is described with Eq. (17):

$$H_k = \left(\begin{array}{cccc} \frac{\partial h(\widehat{x}_k)}{\partial x} & \frac{\partial h(\widehat{x}_k)}{\partial y} & 0 & 0 \end{array} \right) \tag{17}$$

The partial derivatives are given by:

$$\frac{\partial h_N\left(\widehat{x}_k\right)}{\partial x} = \frac{x_0 - x_N}{d_{N,k}} \tag{18}$$

With the Jacobian H of the form 1×6 and the covariance matrix $\widehat{P}_{k|k-1}$ of the form 6×6, the measurement noise variance R can be added as a scalar in a straightforward fashion.

After transferring the measurement model to the measured value and calculating the posteriori state vector, the a posteriori covariance matrix $\widehat{P}_{k|k}$ is computed as follows:

$$\widehat{P}_{k|k} = \left(I - K_k \cdot H_k\right) \cdot \widehat{P}_{k|k-1} \tag{19}$$

The symbol I denotes the identity matrix. With the calculation of the covariance matrix $\widehat{P}_{k|k}$ the time step k of the EKF is completed. In summary, the process of the EKF can be illustrated as in Fig. 11.

4.2 Hardware and Requirements

According to the information in the second section, the environmental parameters in the mine must be considered during the hardware implementation. The UWB modules must be stable and robust enough, so that vibrations and mechanical shocks of the machine, on which the modules are installed, do not affect the physical properties of the module and the measurement results. To achieve this, the most important consideration is a robust housing for all the electrical components to protect them against the mechanical stress. In the presented work, an aluminium enclosure is chosen, which offers IP66 protection according to EN60529 (which determines the ability of an enclosure to protect its contents from

Fig. 11 Position determination using the Extended Kalman Filter
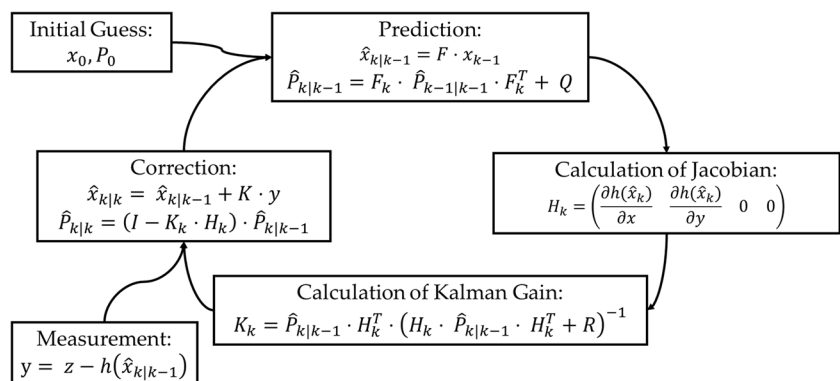
contaminants) and resistance to mechanical stress equal to IK7 [29]. The IP66 standard confirms full protection against dust and protection against strong water jets. To maintain the same IP standard for all mechanical parts, installation of the components inside and on the enclosure must not affect the standard and the components mounted on the housing must also have at least the same standard.

In case of using a metallic housing, a monopole external omnidirectional antenna was used, which was mounted on the top of the enclosure. The developed UWB module is shown in Fig. 12.

Another advantage of the chosen metallic enclosure is its capability to act as a ground plane for the mounted monopole antenna to ensure the antennas transceiving performance. The monopole antennas require a ground plane, whose dimensions are dependent to the antenna length and the wavelength of the transmitted radio signal [30].

4.2.1 Design of the UWB Board

To design a UWB module, a UWB signal generator is required. Therefore, the radio transceiver chip DW1000 by Decawave is chosen, which complies with the IEEE 802.15.4–2011. The IC generates the ultra-wideband signals using the frequency of 38.4 MHz, which will then be emitted as radio signals via the antenna. The UWB transceiver generates the UWB electrical signals as a differential pair, which must be converted to the UWB radio signals. As the required antennas are generally 50 Ω single-ended ones, the 100 Ω differential pair UWB traces must be adapted accordingly, using a wideband balun. To interact with the UWB

transceiver, an onboard microcontroller (STM32 type) with a main clock frequency of 8 MHz and Real Time Clock (RTC) of 32.768 MHz is used. The communication is realized using Serial Peripheral Interface (SPI) between the UWB transceiver and the microcontroller [31]. Figure 13 shows the block diagram of the designed circuit.

The described circuit can be used both as an anchor and tag, as there is no difference between them when using the TWR positioning method. The idea behind this method is the estimation of the Time of Flight of the signal traveling between the transceivers which was explained in Section. 4. The only difference between the modules is found in the software that controls them. When using other positioning techniques, such as AoA or Synchronized TDoA, the anchor and tag require different hardware structures.

The modules can be powered with a 5 V (~ 330 mA) internal battery, 12 V DC external power, or 24 V DC industrial external power, which make it easier to utilize in different applications. Depending on the application, the pre-processed data can be acquired via I^2C, USART, or USB. The developed UWB board is shown in Fig. 14.

Since the module operates in Super High Frequency (SHF) band (3 GHz to 30 GHz), the board is structured in four layers to reduce the size of the highly integrated circuit and to reduce noise especially towards the time and ranging components, with one layer as the ground plane. This also helps to ensure that the signals all have a return path to their sources.

5 Field Measurements

Since mine environments pose special challenges for technical systems in general and especially so for IPS, the development of the system presented requires extensive testing in relevant environment. Testing under laboratory conditions can hardly prove the systems suitability for mining conditions. The designed system has therefore been extensively tested at the former silver mine Reiche Zeche in Freiberg, Germany. This section explains the environmental
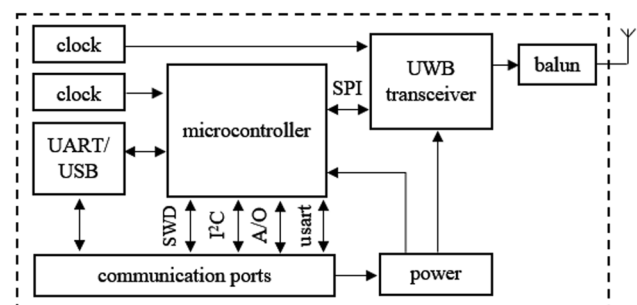

Fig. 12 The developed UWB module including the black outdoor antenna and the blue communication and power supply ports
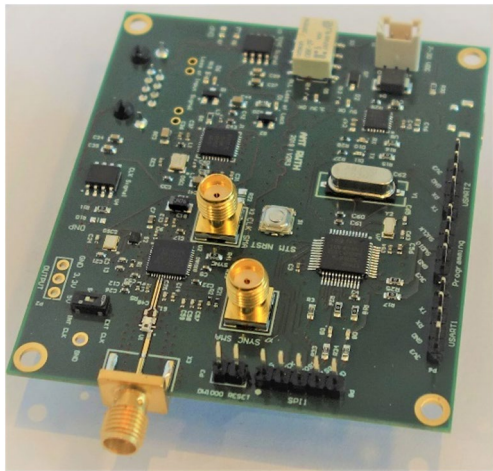

Fig. 13 The block diagram of the UWB module

Fig. 14 The designed UWB module for a TWR positioning system

parameters and the measurement setup. The results and the evaluation of the measurements are discussed in the next section.

As the context of the measurement is the localization of an unmanned ground vehicle (UGV), the measurements are conducted using a robotic vehicle in the test mine. The robot's position is then determined using the UWB technology and positioning algorithms based on the DS-TWR technique.

5.1 Measurement Environment

To test and validate the system, consisting of the developed hardware and software, field measurements are carried out in the underground test mine Reiche Zeche in Freiberg, Germany. The tests are conducted in chosen test area Wilhelm Sthd./Süd on Richtstrecke and Querschlag towards Gangstrecke. Figure 15 shows the measurement area of the mine. It clearly shows the characteristic long and narrow topology of underground mine drifts. The measured distances are about 30 m along each drift and the width of the drift has

been mostly between 2.5 m and 4.5 m. The following section describes the challenges that arise with such topologies.

5.2 Measurement Setup

The goal of this field measurement is to estimate the real-time position of a robotic vehicle. A UWB tag for TWR positioning and an optical prism to obtain a reference position are mounted on the UGV. The stationary anchors are mounted at the walls and roof of the drift and their position measured by the tachymeter is registered. Anchor positions are also referenced in the globally defined coordinate systems of Reiche Zeche.

To verify the measurement results, the position calculated by the UWB system is compared to a reference position measured by a tachymeter (or total station, see Fig. 16). According to vendor specifications, the error in distance is within sub-centimetre range and the error in angle measurement is in the range of milli-gon (mgon). The model used is able to automatically track and measure the position of a reflector in real time, which is mounted to the mobile robot unit to allow real-time reference.

For the given test scenario, the mobile robot unit is navigated in teleoperated mode. The mounted reflector on the vehicle is tracked by the tachymeter for reference, while the measured positions of the UWB system are recorded.

Figure 17 shows the mobile unit with the mounted UWB tag and optical reflector, as well as the remote operator. Figure 18 depicts the setup of the entire system with the tachymeter as reference, the anchor mounted to the wall and the mobile unit carrying tag and reflector.

Figure 19 shows the drift with distributed anchors. For optimal signal reception, the anchors are mounted with the antenna towards the drift. In total, 12 anchors are deployed over two sections of the drift and the intersection area. Table 2 lists the coordinates of the installed anchors in a Cartesian right-handed coordinate system. It is evident that anchors 1 to 5, located in the Querschlag drift, span a length of approximately 27 m in Y direction, but less than 2 m in X

Fig. 15 The area of Wilhelm Sthd./Süd at Reiche Zeche and the chosen testing area
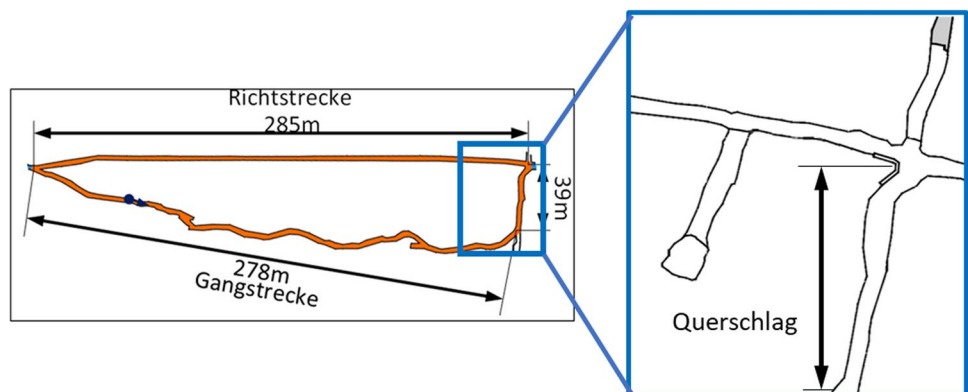
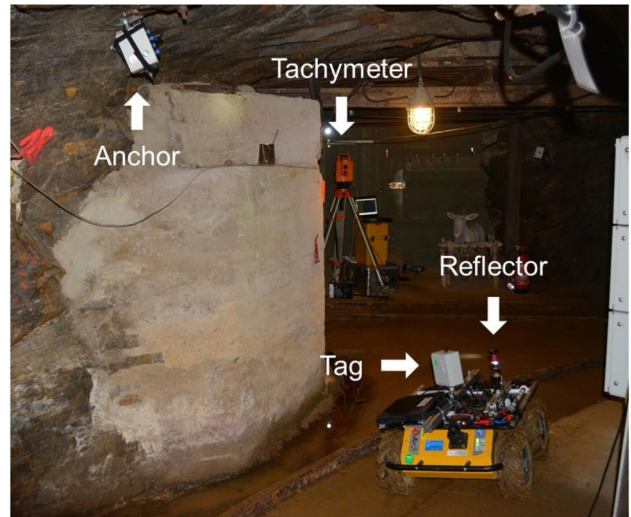**Fig. 16** Tachymeter used in the mine as a reference system

Fig. 17 UGV with reflector, UWB tag, and teleoperator

Fig. 18 The tunnel with the anchors installed on the wall profile and the robotic vehicle containing the UWB tag and a reflector
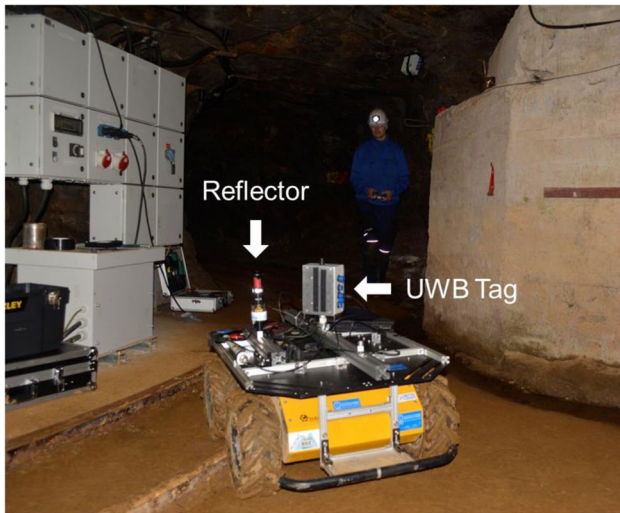

Fig. 19 The mine drift at Reiche Zeche with deployed anchors

direction. This highlights the challenge for localization, as the geometry of the mine drift dictates a setup that is highly vulnerable to the DOP effect as described in Section. 3.5.

The UWB ranging results are transferred from the tag to the connected computer via UART. The position calculation is then performed in real time on the computer within the ROS framework. Thus, the position information is available at the robot. The reference position provided by the tachymeter is read out over a serial port by a connected computer. The raw ranging data, reference position, and UWB position information are logged using the ROS logging tool rosbag.

5.3 Collection of Measurement

Before performing the test, the positions of the installed anchors are measured with the total station placed at the junction to have access to all anchors and the tag. The robot

Table 2 Coordinates of the anchors in metres. The origin of the coordinate system is at the location of the total station

Anchor Nr	X [m]	Y [m]	Z [m]
1	2.26	32.31	0.51
2	0.60	24.43	0.53
3	1.95	17.55	− 0.76
4	0.31	11.58	0.11
5	1.23	5.23	0.44
6	− 3.76	2.99	0.15
7	− 2.15	− 0.13	0.11
8	6.56	− 0.38	0.69
9	12.15	0.84	0.03
10	17.25	− 0.50	− 0.51
11	21.41	1.27	0.18
12	25.64	− 0.17	0.49

moves from the start of the first tunnel at walking speed towards the crossing and then moves to the end of the track in the second tunnel. The position of the tag is determined using trilateration based on DS-TWR. At the same time, the real position of the robot is measured by the tachymeter.

6 Measurement Results and Discussion

This section initially reviews and discusses the system's positioning data and the errors compared to the reference tachymeter. After that, the errors are discussed in the context of the geometric constrains that result in high DOP values perpendicular to the direction of the tunnel.

6.1 Evaluation of Positioning Data and Errors

Figure 20 and Fig. 22 show the raw measurement results of the two test runs from both ends of the area. The reference position is marked in blue and the result of the UWB IPS is marked in red, with the direction of the trajectory marked by the black arrow. Anchor positions are shown in green. All anchor positions as well as the reference position of the UGV are measured by the total station. The reference position as well as the UWB position is thus given in the tachymeter's coordinate system, with the tachymeter

located in the centre at (0, 0, 0). Since the tag is mounted on a floor bound UGV, the horizontal position of the vehicle is of main interest.

Figure 21 and Fig. 22 show the root mean square deviation (RMSE) of the UWB localization from the tachymeter position. A 10-step moving median filter is applied to the recorded time series. This is done to remove individual outliers and to enable better trend recognition. Furthermore, the convergence outliers, which can still be seen in Fig. 20 and Fig. 22, are removed. Data gaps in Fig. 21 and Fig. 23 relate to the phases of the measurement when LOS connection between the tachymeter and the reflector was lost.

Both test runs show varying localization performance with individual outbreaks at different locations. No consistent reference position can be obtained in the direct vicinity of the tachymeter in the root of the coordinate system. This is caused due to physical limitations in the tracking functionality of the tachymeter as well as the steep angle between reflector and tachymeter's objective lens.

In the first test measurement, significant deviations can be found in the beginning of the localization process (Fig. 20). The filter then converges towards plausible values as the tag approaches more anchors. With the progressing path, the localization performance generally looks more stable with errors mostly below 1 m.

Fig. 20 Results of test measurement I plotted in XY plane. The direction of progress is indicated by the black arrow
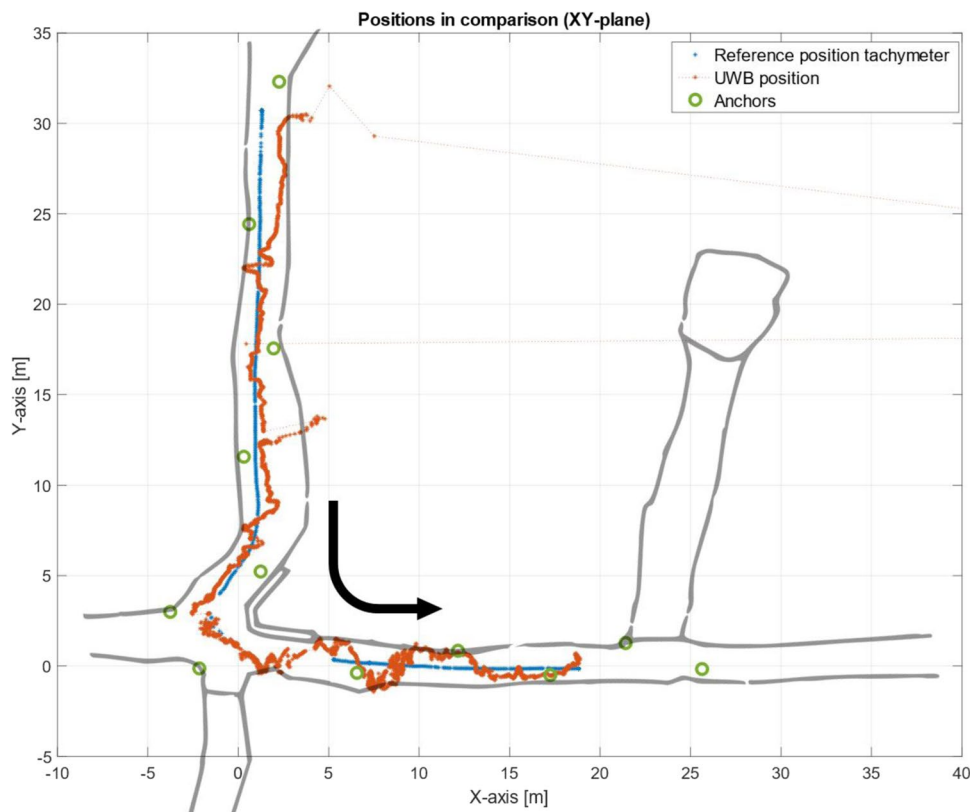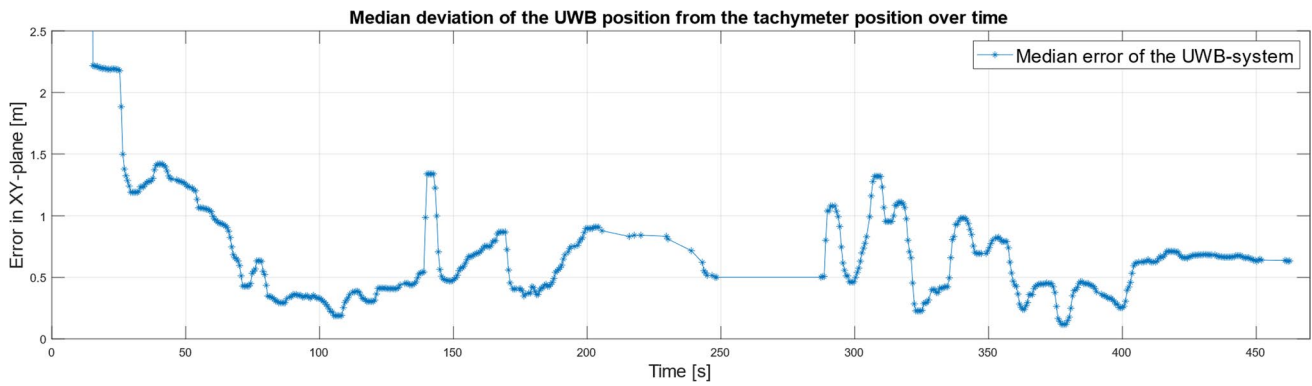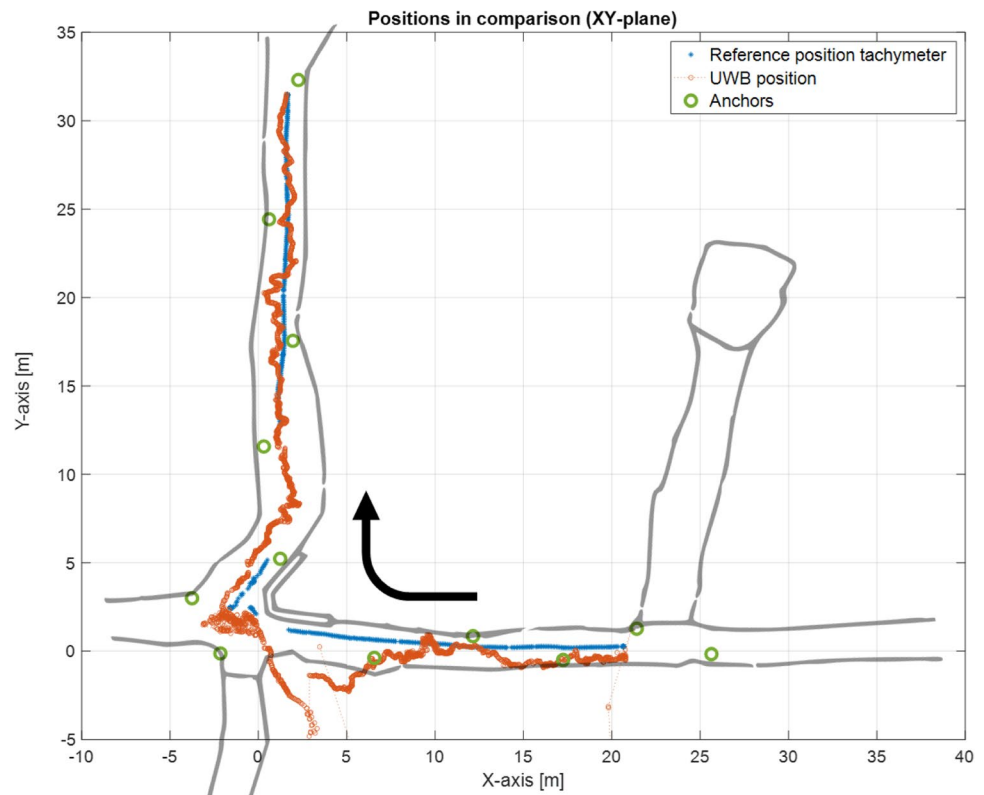
Fig. 21 Localization error of UWB system over time during test measurement I with applied 10-step moving median

Fig. 22 Results of test measurement II plotted in XY plane. The direction of progress is indicated by the black arrow

6.2 Evaluation of DOP Influence on the Conducted Tests

Further significant deviations are found in both cases as the vehicle approaches the junction of the drifts. Figure 20 and Fig. 22 clearly show how NLOS situations with massive rock walls occur in the intersection area. While LOS conditions between tag and anchors can be expected along most parts of the drift, the intersection area proves to be a critical zone. Figure 21 and Fig. 23 support this presumption. Both graphs show instable phases before or after traversing the intersection, more precisely near coordinates (0, 12) in

measurement I and around coordinates (6, 0) in measurement II. The scheme in both cases is similar, as the UWB position jumps significantly and then converges back to more reasonable position estimations. Presumably, this behaviour might be caused by reflected or noisy signals from distant or NLOS anchors, that are received as the UGV approaches the junction, and which then are received in an increasingly clearer fashion as the trajectory progresses.

From visual inspection of Fig. 20 and Fig. 22, the larger outbreaks of positioning error mainly seem to occur perpendicular to the main direction of the tunnel. Localization robustness in this direction seems to be significantly lower
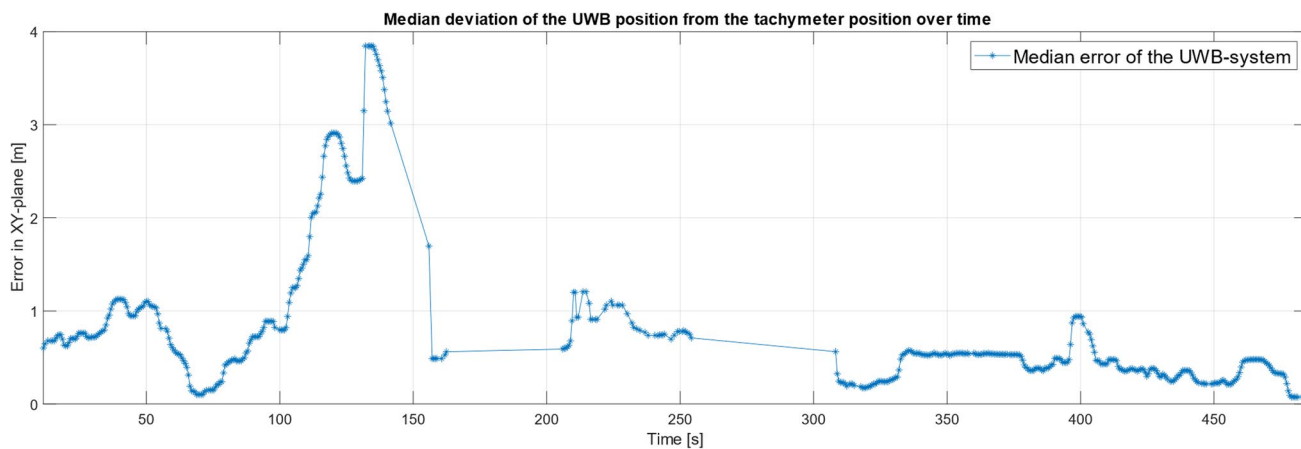
Fig. 23 Localization error of UWB system over time during test measurement II with applied 10-step moving median

and more susceptible to erroneous signals. Figures 20, 21, 22, and 23 however cannot ultimately prove this presumption, because the UWB and tachymeter trajectories cannot be set in a timely relation in a precise sub second manner with each other. The higher errors perpendicular to the tunnel are therefore investigated in detail in Section. 6.2. The localization results presented in Section. 6 point to the presumption that the localization error occurs mainly perpendicular to the main heading of the drift. This is in accordance with the hypothesis of high DOP influence from Section. 3.5. Thus, the DOP value for the given measurement setup is calculated for the reference position over time. The derivation and calculation of the DOP value is summarized in Section. 3.5 and explained in detail in Zwirello et al. [15]. Figure 24 shows the 10-step median DOP values along X and Y axis (XDOP and YDOP) of the tachymeters coordinate system. With the direction of the trajectory from Fig. 20 taken into consideration, the presumption of DOP influence is substantiated. As expected, the DOP influence on the position along the X direction is high during the first half of the measurement (in Querschlag), where anchor positions were very narrow in X

direction. With the shift in direction towards the second drift (Richtstrecke), YDOP values increased significantly while XDOP values decreased. Although the rating of DOP influence on positioning results is not standardized, and literature sources like [2] and [32] deviate in their evaluations, DOP values between 3 and 5 are mostly regarded as the lower bound of what is acceptable for GPS localization. IPS however usually has higher requirements regarding the DOP due to lower ranging accuracy in comparison to GPS.

To further investigate the influence of the anchor installation on localization performance, the localization error in X and Y direction is plotted over time. Figure 25 shows the median deviation of the UWB position from the reference position in X and Y direction over time. It can be observed how the localization error in X direction is mostly larger while the tag is still in the Querschlag drift and how the error decreases during the second half (in Richtstrecke), while the error in Y direction behaves the opposite. Accordingly, Fig. 25 confirms the presumption from Section. 6 that the system is particularly susceptible to localization error in perpendicular direction to the drift heading. Major breakouts
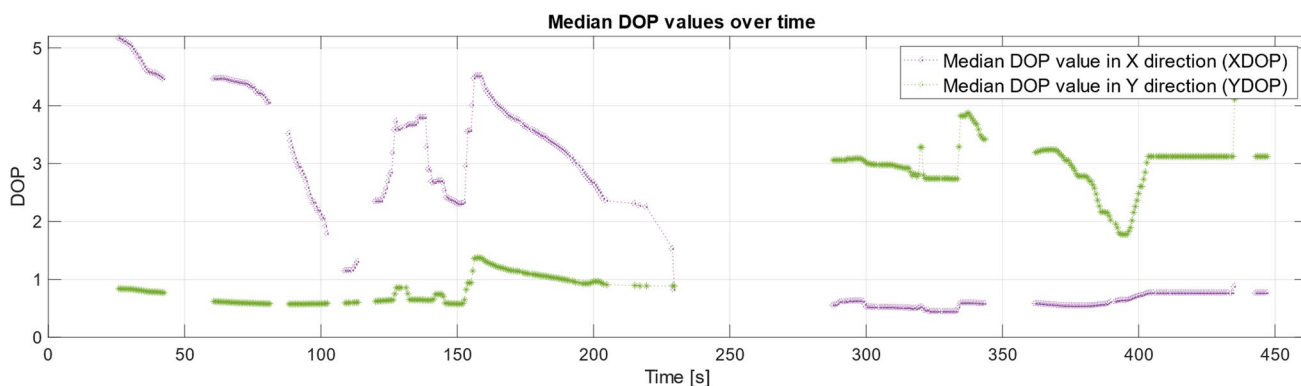

Fig. 24 10-step median DOP Values along X and Y axis during test measurement I over time
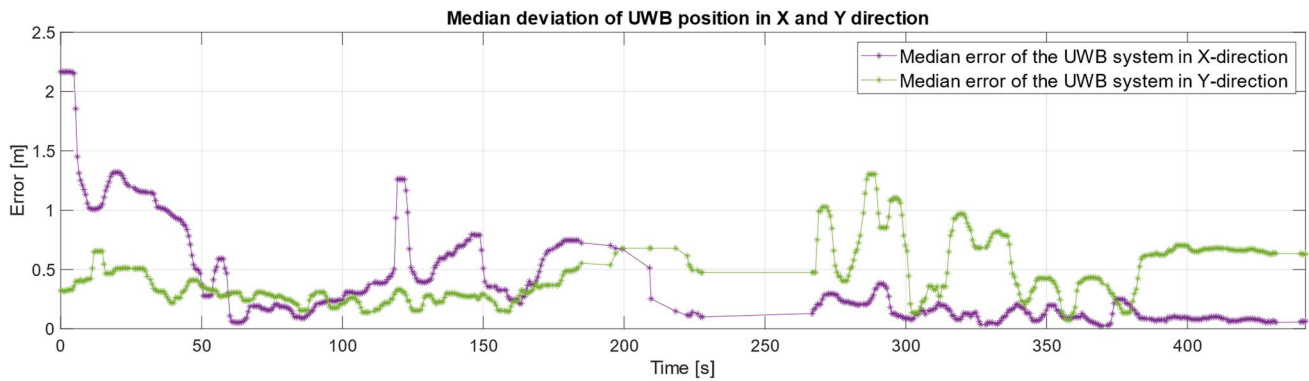
Fig. 25 Median Deviation of UWB position in X and Y direction as measured in measurement I

mostly occur in that direction, while localization robustness along the tunnel is significantly higher. In the context of the intersection area breakouts, it now becomes clear that the breakouts are caused by faulty range measurements, which are amplified by DOP. The analysis of DOP and error behaviour therefore substantiates the hypothesis of DOP influence (and thus anchor constellation) as a major impairment on the localization performance in the given application.

The test environment of Reiche Zeche is an extreme example in terms of spatial confinement. Modern mining operations employ heavy machinery in underground environments, which require larger drift diameters and in turn allow for more appropriate anchor placement. For modern, operational mine environments, the impact of the DOP effect is thus expected to be less significant. In an operational context, the systems accuracy is sufficient for equipment tracking. Regarding the automation of mobile equipment, a more robust localization is required, especially transverse to the tunnel heading. This could potentially be achieved by vehicle dynamic constrains and plausibility considerations in filtering, as these transverse outbreaks result in implausible movements and positions outside of the mine drift.

7 Discussion and Outlook

Accurate positioning information is a central step in the process of increasing automation and digitalization in the mining industry, yet GNSS coverage is categorically not available in underground mines. Underground environments present a variety of special challenges for radio-based IPS. Massive rock walls cause signal blockage and multipath effects, while the geometric conditions of drifts set limits on the deployment of base stations. Moisture, dust, heat, and mechanical shock or stress raise additional requirements for the electrical hardware.

The system developed, consisting of hardware and software, is described in this article. The localization of a mobile robot using UWB radio technology in an underground environment is presented in this paper. Due to its physical properties, UWB is regarded to be the best choice among established localization technologies. On the one hand, the working frequency band is in the field of SHF range, which requires additional demands on the implementation of an appropriate module. On the other hand, considering the environmental parameters in the mine, appropriate hardware such as enclosure, antenna, and communication ports must be taken into account, which are robust and do not impair the functionality of the system.

To avoid costly and complicated time synchronization issues between the participants in the system, the Double-Sided Two-Way Ranging localization method was implemented. An Extended Kalman Filter was used for the multilateration process.

Two test measurements were conducted in the former silver mine Reiche Zeche in Freiberg, Germany. Despite challenging environmental conditions, promising positioning results were achieved. Both test measurements showed localization error predominantly below 1 m, with isolated outbreaks with significantly higher positioning error. Outbreaks mostly occurred in the vicinity of the drift intersection, which suggests that noisy signals are received from non-line of sight anchors around massive rock corners. Overall, the test results showed sufficient accuracy for equipment tracking in process analysis and operation control.

Due to the narrow geometry of the drifts and, consequently, the narrow placement of anchors, the Dilution of Precision (DOP) effect is suspected to have significant influence on the localization performance. An analysis of the DOP effect along X and Y direction supported this assumption, as DOP values perpendicular to the main axis of the tunnel are generally higher. Additionally, a comparison between DOP values along one axis and the respective positioning error in the same axis strongly indicates influence of DOP on the positioning error. Furthermore, the most significant outbreaks mainly occurred perpendicular

to drift heading. The sub-optimal anchor placement is thus suspected to have negatively impacted the positioning performance.

7.1 Areas for Future Work

The results of this work have clearly shown the challenges for IPS that arise due to difficult environments, and which need to be overcome by an IPS for underground mines. In particular, the challenges of a narrow anchor setup became clear. Additionally, tests with a higher number of anchors have shown the requirement to select the anchors more carefully for positioning updates. Anchors, which deteriorate the position estimation due to bad signals or NLOS conditions, should be discarded by the algorithm. This issue will be addressed in future development steps.

Nevertheless, promising positioning results could be obtained under difficult conditions, which allow for example the tracking of equipment for process analysis and monitoring. For certain collision avoidance or automation scenarios however, positioning accuracy in the magnitude of a few decimetres in error could be required. Both test measurements have shown that in this case an improvement in accuracy and reliability of the localization are required. With respect to vehicle automation, geometric and dynamic vehicle constraints in filtering and a combination of the UWB system with additional (existing) sensors should be considered. Furthermore, sudden outbreaks in the positioning result suggest highly non-Gaussian noise distribution, for which an Extended Kalman Filter is not an optimal estimator. An item of future work is implementation and testing of different positioning algorithms that show enhanced performance under nonlinear conditions.

Data Availability Not applicable for this publication.

Code Availability Not applicable for this publication.

Declarations

Ethics Approval Not applicable for this publication.

Consent to Participate Not applicable for this publication.

Consent for Publication All authors whose names appear on the submission have full consent for this publication and agree to be accountable for all aspects of the work in ensuring that questions related to the accuracy or integrity of any part of the work are appropriately investigated and resolved.

Conflict of Interest The authors declare no competing interests.

References

1. Clausen E, Lehnen F, Sörensen A, Uth F, Mitra R, Schwarze B (2020) Assessment of the Effects of Global Digitalization Trends on Sustainability in Mining Part II. Bundesanstalt für Geowissenschaften und Rohstoffe, Hannover
2. Neumann K (2016) Ultra-Wideband-Technologie für den Einsatz im Schwermaschinenbau, Aachen: Dissertation, RWTH Aachen
3. Kianfar AE, Uth F, Baltes R, Clausen E (2020) Development of a Robust Ultra-Wideband Module for Underground Positioning and Collision Avoidance. Min, Metall Explor 37(6):1821–1825
4. Thrybom L, Neander J, Hansen E, Landernäs K (2015) Future Challenges of Positioning in Underground Mines. IFAC-PapersOnLine 48(10):222–226
5. Zheng X, Wang B, Zhao J (2019) High-precision positioning of mine personnel based on wireless pulse technology. Plos One 14(7):e0220471
6. Alarifi A, Al-Salman AM, Alsaleh M, Alnafessah A, Al-Hadhrami S, Al-Ammar MA, Al-Khalifa HS (2016) "Ultra Wideband Indoor Positioning Technologies: Analysis and Recent Advances. Sensors 16(50):707
7. Zare M, Battulwar R, Seamons J, Sattarvand J (2021) Applications of Wireless Indoor Positioning Systems and Technologies in Underground Mining: a Review. Min, Metall Explor 38(6):2307–2322
8. Seguel F, Palacios-Játiva P, Azurdia-Meza C, Krommenacker N, Charpentier P, Soto I (2022) Underground mine positioning: A review. IEEE Sens J 22(6):4755–4771
9. Barua B, Kandil N, Hakem N (2018) On Performance Study of TWR UWB Ranging in Underground Mine. Sixth International Conference on Digital Information, Networking, and Wireless Communications (DINWC). Beirut, Lebanon
10. Cao B, Wang S, Ge S, Ma X, Liu W (2020) A Novel Mobile Target Localization Approach for Complicate Underground Environment in Mixed LOS/NLOS Scenarios. IEEE Access 8:96347–96362
11. Cao B, Wang S, Ge S, Liu W (2020) Improving Positioning Accuracy of UWB in Complicated Underground NLOS Scenario Using Calibration, VBUKF, and WCA. IEEE Trans Instrum Meas 70:1–13

12. Molnár M, Luspay T (2020) Development of an UWB based Indoor Positioning System. 28th Mediterranean Conference on Control and Automation (MED)

13. Ding G, Lu H, Bai J, Qin X (2020) Development of a High Precision UWB/Vision-based AGV and Control System,. 5th International Conference on Control and Robotics Engineering

14. Li M-G, Zhu H, You S-Z, Tang C-Q (2020) UWB-Based Localization System Aided With Inertial Sensor for Underground Coal Mine Applications. IEEE Sens J 20:6652–6669

15. Zwirello L (2013) Realization Limits of Impulse-Radio UWB Indoor Localization Systems, Karlsruhe: Dissertation, Karlsruher Institut für Technologie

16. Scholtz R, Pozar D, Won N (2005) Ultra-Wideband Radio. EURASIP Journal on Advances in Signal Processing

17. Win MZ, Dardari D, Molisch AF, Wiesbeck W, Zhang J (2009) History and applications of UWB. Proc IEEE 97(2):198–204

18. European Commission, "European Commission decision on the harmonisation of radio spectrum for equipment using ultra-wideband technology in the Union and repealing Decision," 14 May 2019. [Online]. Available: https://eur-lex.europa.eu/legal-content/EN/TXT/?uri=uriserv%3AOJ.L_.2019.127.01.0023.01.ENG&toc=OJ%3AL%3A2019%3A127%3ATOC.

19. Institute of Electrical and Electronics Engineers (IEEE) (2012) "IEEE Standard for local and metropolitan area networks — Part 15.4: Low-Rate Wireless Personal Area Networks (LR-WPANs),"

20. Sahinoglu Z, Gezici S, Güvenc I (2011) Ultra-wideband positioning systems: Theoretical limits, ranging algorithms, and protocols. Cambridge University Press

21. DecaWave Ltd (2015) "UWB Regulations, A Summary of Worldwide Telecommunications Regulations governing the use of Ultra-Wideband radio," DecaWave Ltd.

22. Yavari M (2015) Indoor Real-Time Positioning Using Ultra-Wideband Technology. University of New Brunswick, Thesis

23. Zou Z (2011) Impulse Radio UWB for the Internet-of-Things: A Study on UHF/UWB Hybrid Solution. Stockholm: Dissertation, Universitetsservice US AB

24. Deepak V, Kumar S, Katabi D (2015) Sub-nanosecond time of flight on commercial Wi-Fi cards, SIGCOMM 2015 - Proceedings of the 2015 ACM Conference on Special Interest Group on Data Communication 45(4):121–122

25. Zandian R (2019) Ultra-wideband based indoor localization of mobile nodes in ToA and TDoA configurations. Bielefeld: Dissertation, Universität Bielefeld

26. McElroy C, Neirynck D, McLaughlin M (2014) Comparison of wireless clock synchronization algorithms for indoor location systems, in 2014 IEEE International Conference on Communications Workshops (ICC), Sydney, Australia

27. Niestroj C (2019) Performance und Potential eines untertägigen Lokalisierungssystems auf Basis der Ultra-wideband Funktechnologie, Aachen: Dissertation. RWTH Aachen University, 2019

28. Khan R, Sottile F (2012) Hybrid positioning through extended Kalman filter with inertial data fusion. Int J Inf Electron Eng 3

29. ROSE-Systemtechnik-GmbH (2020) "Aluminium Druckgussgehäuse," *Technical report*.

30. Weiner M (2003) Monopole Antennas, Taylor & Francis

31. Decawave Ltd (2015) "DW1000 Datasheet," Decawave Ltd., Ireland.

32. Isik O, Hong J, Petrunin I (2020) Integrity Analysis for GPS-Based Navigation of UAVs in Urban Environment. MDPI Robotics 9(3):66